

Quantifying noise in ultrafast laser sources and its effect on nonlinear applications

Vadim V. Lozovoy,¹ Gennady Rasskazov,¹ Dmitry Pestov,³ and Marcos Dantus^{1,2,3,*}

¹Department of Chemistry, Michigan State University, East Lansing, Michigan 48824, USA

²Department of Physics and Astronomy, Michigan State University, East Lansing, Michigan 48824, USA

³Biophotonic Solutions, 1401 East Lansing Dr., Suite 112, East Lansing, Michigan USA 48823, USA
dantus@msu.edu

Abstract: Nonlinear optical applications depend on pulse duration and coherence of the laser pulses. Characterization of high-repetition rate pulsed laser sources can be complicated by their pulse-to-pulse instabilities. Here, we introduce and demonstrate experimentally a quantitative measurement that can be used to determine the pulse-to-pulse fidelity of ultrafast laser sources. Numerical simulations and experiments illustrate the effect of spectral phase and amplitude noise on second and third harmonic generation.

©2015 Optical Society of America

OCIS codes: (320.7100) Ultrafast measurements; (320.5520) Pulse compression; (320.5540) Pulse shaping.

References and links

1. W. Denk, J. H. Strickler, and W. W. Webb, "Two-photon laser scanning fluorescence microscopy," *Science* **248**(4951), 73–76 (1990).
2. P. Xi, Y. Andegeko, L. R. Weisel, V. V. Lozovoy, and M. Daunts, "Greater signal, increased depth, and less photobleaching in two-photon microscopy with 10 fs pulses," *Opt. Commun.* **281**(7), 1841–1849 (2008).
3. R. C. Greenhow and A. J. Schmidt, *Picosecond Light Pulses*, vol.2 (Advances in Quantum Electronics, 1974).
4. R. Trebino, *Frequency-Resolved Optical Gating: The Measurement of Ultrashort Laser Pulses* (Kluwer Academic Publishers, 2002).
5. C. Iaconis and I. A. Walmsley, "Spectral phase interferometry for direct electric-field reconstruction of ultrashort optical pulses," *Opt. Lett.* **23**(10), 792–794 (1998).
6. J. Ratner, G. Steinmeyer, T. C. Wong, R. Bartels, and R. Trebino, "Coherent artifact in modern pulse measurements," *Opt. Lett.* **37**(14), 2874–2876 (2012).
7. M. Rhodes, G. Steinmeyer, J. Ratner, and R. Trebino, "Pulse-shape instabilities and their measurement," *Laser Photonics Rev.* **7**(4), 557–565 (2013).
8. Y. Li, L. F. Lester, D. Chang, C. Langrock, M. M. Fejer, and D. J. Kane, "Characteristics and instabilities of mode-locked quantum-dot diode lasers," *Opt. Express* **21**(7), 8007–8017 (2013).
9. J. N. Ames, S. Ghosh, R. S. Windeler, A. L. Gaeta, and S. T. Cundiff, "Excess noise generation during spectral broadening in a microstructured fiber," *Appl. Phys. B* **77**(2-3), 279–284 (2003).
10. M. Horowitz, Y. Barad, and Y. Silberberg, "Noiselike pulses with a broadband spectrum generated from an erbium-doped fiber laser," *Opt. Lett.* **22**(11), 799–801 (1997).
11. B. Nie, G. Parker, V. V. Lozovoy, and M. Daunts, "Energy scaling of Yb fiber oscillator producing clusters of femtosecond pulses," *Opt. Eng.* **53**(5), 051505 (2014).
12. D. E. McCumber, "Intensity fluctuations in the output of cw laser oscillators. I," *Phys. Rev.* **141**(1), 306–322 (1966).
13. M. C. Cox, N. J. Copner, and B. Williams, "High sensitivity precision relative intensity noise calibration standard using low noise reference laser source," *IEE P. - Sci. Meas. Tech.* **145**(4), 163–165 (1998).
14. S. A. Diddams, M. Kirchner, T. Fortier, D. Braje, A. M. Weiner, and L. Hollberg, "Improved signal-to-noise ratio of 10 GHz microwave signals generated with a mode-filtered femtosecond laser frequency comb," *Opt. Express* **17**(5), 3331–3340 (2009).
15. A. F. J. Runge, C. Aguergaray, N. G. R. Broderick, and M. Erkintalo, "Coherence and shot-to-shot spectral fluctuations in noise-like ultrafast fiber lasers," *Opt. Lett.* **38**(21), 4327–4330 (2013).
16. T. Pfeifer, Y. Jiang, S. Düsterer, R. Moshhammer, and J. Ullrich, "Partial-coherence method to model experimental free-electron laser pulse statistics," *Opt. Lett.* **35**(20), 3441–3443 (2010).
17. V. V. Lozovoy, B. Xu, Y. Coello, and M. Dantus, "Direct measurement of spectral phase for ultrashort laser pulses," *Opt. Express* **16**(2), 592–597 (2008).
18. Y. Coello, V. V. Lozovoy, T. C. Gunaratne, B. Xu, I. Borukhovich, C.-H. Tseng, T. Weinacht, and M. Dantus, "Interference without an interferometer: a different approach to measuring, compressing, and shaping ultrashort

- laser pulses,” J. Opt. Soc. Am. B **25**(6), A140–A150 (2008).
19. M. Miranda, C. L. Arnold, T. Fordell, F. Silva, B. Alonso, R. Weigand, A. L’Huillier, and H. Crespo, “Characterization of broadband few-cycle laser pulses with the d-scan technique,” Opt. Express **20**(17), 18732–18743 (2012).
20. V. Loriot, G. Gitzinger, and N. Forget, “Self-referenced characterization of femtosecond laser pulses by chirp scan,” Opt. Express **21**(21), 24879–24893 (2013).
-

1. Introduction

Applications such as two-photon excited fluorescence microscopy and second harmonic generation (SHG) imaging depend on pulse duration [1,2]. Pulse duration can therefore be an important criterion for predicting the expected nonlinear optical signal when comparing different laser sources. Unfortunately, pulse characterization of noisy or partially incoherent laser sources is challenging given the appearance of the so-called autocorrelation coherent artifact [3]. In a recent publications, frequency resolved optical gating (FROG) [4] and spectral phase interferometry for direct electric-field reconstruction (SPIDER) [5] were evaluated for their ability to quantify pulse shape instabilities [6–8]. The growing number of ultrafast laser sources that take advantage of self-phase modulation to increase spectral bandwidth, a process that in some cases leads to phase and amplitude noise, raise the question of how to accurately characterize their output based on averaged measurements. Microstructured fibers, for example, have been used to generate short pulses; however, the pulse-to-pulse reproducibility may be compromised [9]. Some fiber lasers are known to operate in both soliton-like and noise-like regimes [10, 11], quantifying noise and its impact on practical nonlinear optical applications is therefore a high-priority endeavor. In this paper we introduce a measurement that can be used to determine the pulse-to-pulse fidelity of a laser, which quantifies the performance of the laser for nonlinear optical processes and helps distinguish between spectral phase and spectral amplitude fluctuations, when the laser spectrum changes from pulse to pulse.

Previous indicators of laser performance include basic techniques for measuring the amplitude noise or relative intensity fluctuations of continuous wave lasers [12, 13]. Some methods have evolved to measure the noise and jitter of metrology sources, where it becomes important to know how close the source’s contribution is to the noise floor [14]. More recently, the shot-to-shot coherence and spectral fluctuations of noise-like ultrafast fiber lasers was characterized making use of Young’s-type interference and single shot spectrometry at megahertz rates [15]. Such measurements showed clearly the lack of coherence in noise-like pulse trains. The metric presented here and referred to as *fidelity* is best suited to characterize laser sources being used for nonlinear applications, using tools usually found in an ultrafast laser laboratory. The fidelity of a pulsed laser is an indicator of expected statistically-averaged laser performance. Fidelity is insensitive to intensity fluctuations, which are easily measured by a simple photodiode. Given two laser sources with similar transform-limited (TL) pulse duration (based on averaged laser spectra), repetition rate and energy per pulse, the one with higher fidelity will lead to more efficient SHG and brighter multiphoton microscopy images.

2. Theoretical concept

It is tempting to tie expected laser performance to average pulse duration; unfortunately, measuring the average pulse duration of a noisy laser by conventional methods such as autocorrelation is not reliable because of the aforementioned coherent spike. The duration of the spike depends on the coherence time τ_c of the source, defined by the spectral width and shape of the pulse. Here we define fidelity based on the attenuation of a nonlinear optical process such as SHG as a function of added linear chirp, later we discuss other nonlinear optical processes such as third-harmonic generation (THG).

We introduce an expression that can be used in the laboratory to determine the pulse-to-pulse fidelity function or curve as defined by Eq. (1)

$$\langle F(\phi'') \rangle = \frac{I_{\phi''}^{SHG} / I_{TL}^{SHG}}{\langle I_{\phi''}^{SHG} \rangle / \langle I_{\phi''=0}^{SHG} \rangle}, \quad (1)$$

where ϕ'' is the amount of chirp in the frequency domain. The intensities in the numerator are calculated assuming coherent noiseless pulses with a spectrum identical to the averaged laser spectrum being characterized. The denominator corresponds to averaged values measured for the second harmonic intensity of the laser source for the case where the pulse has an amount ϕ'' of linear chirp, divided by the second harmonic intensity when the output has no added chirp. The ratio between the averaged measurements makes the measurement insensitive to simple intensity fluctuations. Note that a noisy ensemble of pulses, with low fidelity, produces more SHG than one with high fidelity in the presence of a large chirp. This is because the low-fidelity source, on average, has pulses that are longer than the coherence time τ_c and, therefore, is less affected by chirp. Thus a laser output with $\langle F \rangle \approx 1$ is highly coherent, while one with $\langle F \rangle \approx 0$ is incoherent. The key is that Eq. (1) can be used to determine the practical performance of a laser, whilst avoiding the coherent artifact that is inherent to autocorrelation measurements. For large chirp values the intensity of nonlinear optical processes like SHG divided by the intensity of the same pulse when TL decays as $1/|\phi''|$. Therefore Eq. (1) reaches asymptotically a value for large chirp values $|\phi''| \gg \tau_c^2$. The definition above considers pulse trains that average to Fourier-limited pulses, measurements on non-Fourier-limited pulses are discussed later in the manuscript.

3. Numerical simulations

Armed with a functional measurement for fidelity we test a number of possible sources of noise that may be found in ultrafast lasers. In all cases we consider conditions that affect individual pulses but are difficult to detect by averaged measurements. In particular we considered (a) spectral jitter, where the spectrum experiences small random shifts towards shorter or longer wavelengths that average to zero; (b) random positive and negative chirp values that average to zero; (c) random high-order phase distortions that average to zero; (d) random phases on pulses that have random spectral amplitudes that satisfy a certain temporal window. The longer the temporal window used the lower the fidelity. Cases *a-c* can be found in oscillators, especially when operating at high pumping powers and in the presence of small air fluctuations. Case (d) is unusual for oscillators but has been found in the generation of ultrafast pulses from free-electron lasers [16] and has been used to simulate noisy pulses [6,7].

For each simulation we generate a train of 100 ‘noisy’ pulses, and calculate their corresponding averaged characteristics including fundamental spectrum and SHG spectrum as a function of linear chirp introduced. From this data we calculated their fidelity as a function of chirp introduced according to Eq. (1). For each case we varied the noise magnitude to simulate output with fidelity values that ranged from 0.1 to 1.0. For all cases we compared with ideal transform-limited 36 fs pulses. When calculating the train of noisy pulses we made sure that on average they had no phase distortion; that is, any pulse characterization method that measured their average phase would indicate they are transform limited.

If one introduces linear chirp and collects the SHG spectrum at the same time, one obtains a chirp-scan. Chirp scans have been shown to provide accurate pulse characterization, especially when one considers the linear chirp introduced as a reference phase [17–20]. The chirp-scan, or multiphoton intrapulse interference phase scan (MIIPS), provides a direct measurement of the second derivative of the spectral phase [17]. Such scans are presented below for a set of ideal 36 fs pulses and for noisy pulses obtained by applying a random amount of positive or negative chirp, see Fig. 1. The maximum SHG intensity at zero chirp observed for both cases indicates both sets of pulses have no systematic spectral phase such as

linear chirp or third order dispersion. The ensemble of noisy pulses, however, shows a much broader distribution of intensities because within the ensemble are pulses with a wide range of chirp values.

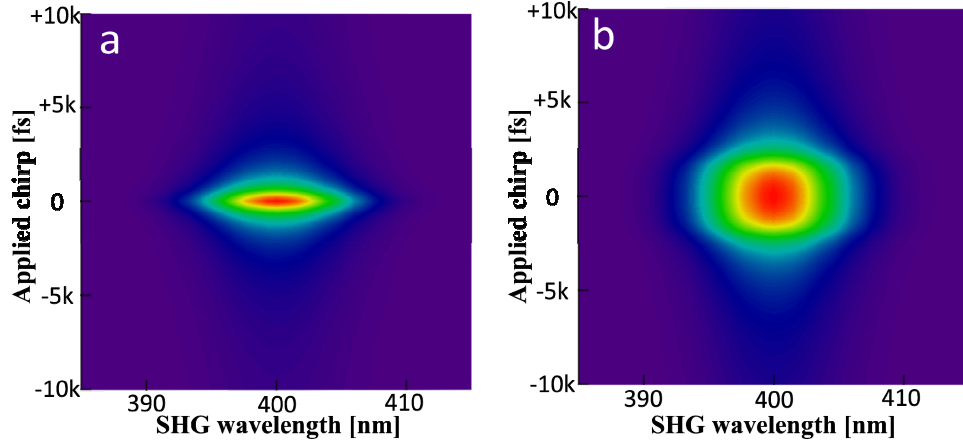


Fig. 1. Numerical simulations of a MIIPS scan, where the SHG spectrum is plotted as a function of chirp, obtained for an ideal ensemble of coherent 36 fs transform-limited pulses with unit fidelity (a) and for an ensemble of noisy pulses with random amounts of positive and negative chirp (b). The SHG spectrum in both cases is the average of the entire ensemble of pulses.

From the simulations shown in Fig. 1, it is possible to calculate fidelity. We present such analysis for an ensemble of pulses having random magnitudes of positive and negative linear chirp such that the asymptotic fidelity equals 0.5. In Fig. 2(a) we show how SHG intensity varies for ideal pulses (dashed line) and for the ensemble of noisy pulses (bold line) as a function of introduced linear chirp. Note that the noisy train of pulses is less sensitive to linear chirp. Figure 2(b) corresponds to the reciprocal dependence shown in Fig. 2(a) showing that for large chirp the dependence of SHG on chirp becomes linear. The fidelity curve and asymptotic value $\langle F \rangle$, as defined by Eq. (1) is shown in Fig. 2(c).

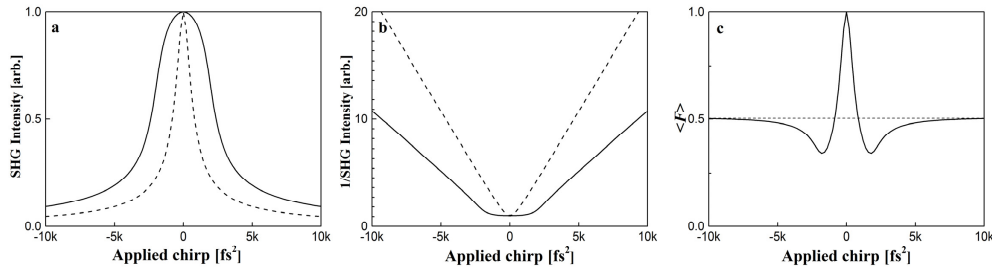


Fig. 2. Numerical simulations corresponding to Fourier-limited (dashed line) and noisy pulses (solid line) having a distribution of positive and negative chirps; see text. The dashed line in Fig. 1(c) indicates the asymptotic fidelity.

We now examine in more detail signatures from different types of noise. For example, we illustrate spectral amplitude noise Fig. 3(top), random spectral phase noise Fig. 3(middle) and a mixture of phase and amplitude noise Fig. 3(bottom). We find that the fidelity curve is distinctively different depending on the source of noise. Amplitude noise results in an averaged spectrum that is broader that would correspond to shorter pulses. This leads to a sharp feature in the fidelity curve, see Fig. 3(top). For the case of random phase noise, pulses are much less sensitive to small amounts of chirp given the additional phase modulation. This leads to the appearance of features below the asymptotic fidelity value, see Fig. 3(middle).

The fidelity curves are instrumental to determine if the source of noise is phase or amplitude spectral fluctuations (the spectrum changes from pulse to pulse). For completion, we give a case in which the noise comes from both amplitude and phase fluctuations Fig. 3(bottom). In this case the central feature in the fidelity curve is broad.

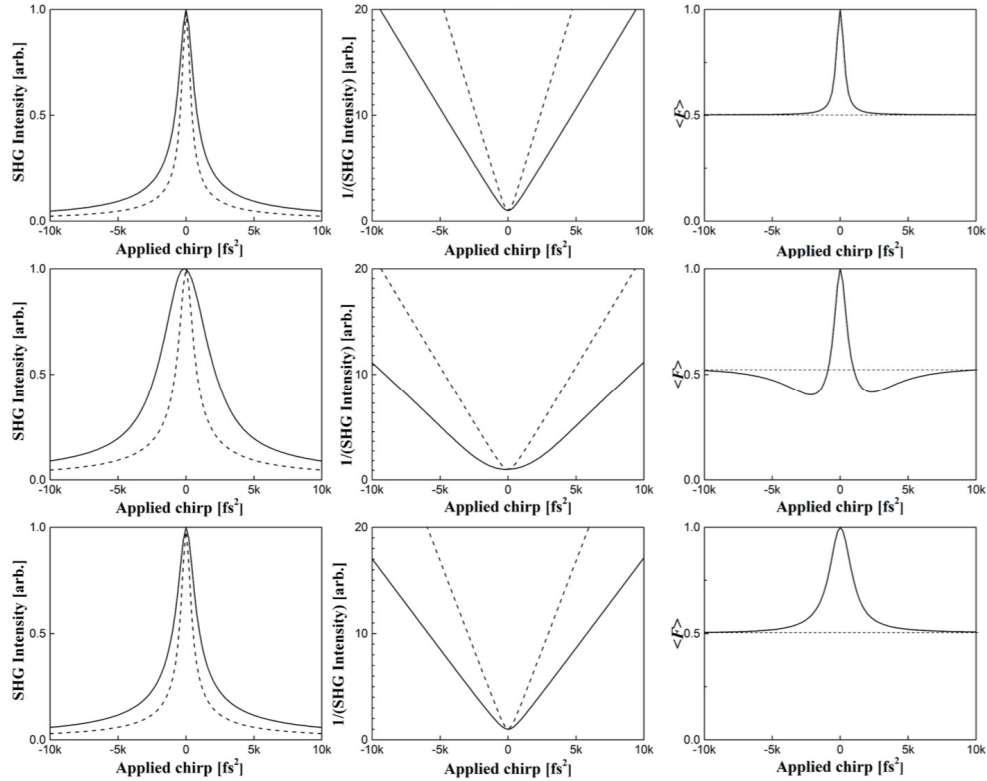


Fig. 3. Numerical simulations corresponding to Fourier-limited (dashed line) and noisy pulses (solid line) having (top) spectral jitter, (middle) random phase modulations, and (bottom) a mixture of phase and amplitude modulations. The dashed line in the third column indicates the asymptotic fidelity.

It is important to determine how a fidelity value translates into practical applications such as two-photon excited fluorescence or SHG imaging. The correlation between fidelity (x -axis) and relative intensity of SHG or THG are plotted in Fig. 4. We have found that the source of noise changes the dependence; therefore, we introduce Eq. (2).

$$\langle I_{\phi^* \neq 0}^{SHG} \rangle = I_{TL}^{SHG} \langle F(\phi^n) \rangle^n \quad (2)$$

where the SHG or THG attenuation experienced by the ensemble of pulses compared to a fully coherent source depends on the asymptotic fidelity value to the n th power. The asymptotic fidelity value can be used to determine the effective attenuation or nonlinear optical signal caused by noise. The power dependence, n , in Eq. (2) depends from the type of noise and nonlinear optical process as shown in Fig. 4. For spectral amplitude noise SHG/THG intensity correlates with fidelity to the $n = 0.5/n = 1$. For phase and amplitude noise SHG/THG correlates with fidelity to the order $n = 0.6-0.7/n = 1.5$. For phase noise SHG/THG correlates with fidelity to the order $n = 1/n = 2$. Measuring a fidelity curve, Eq. (1), reveals the dominant contribution to noise (phase or amplitude). The asymptotic fidelity value obtained for large chirp tells us, through Eq. (2), by how much a nonlinear process such as SHG or THG is attenuated because of noise.

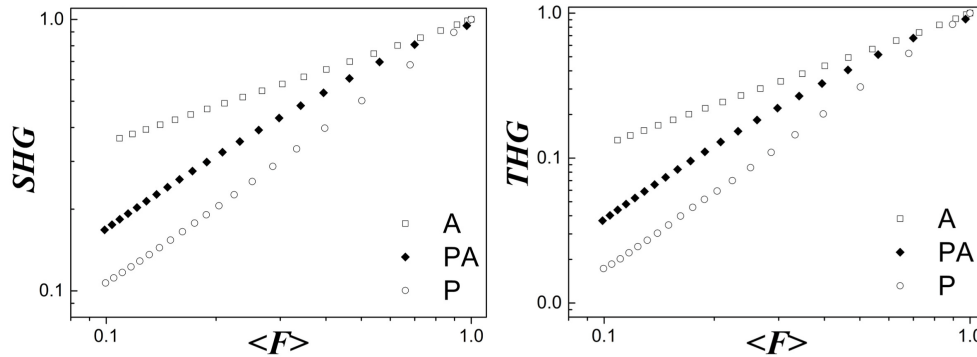


Fig. 4. Numerical simulations showing the power dependence of expected SHG and THG intensity on fidelity: A. for amplitude noise, PA for phase and amplitude noise, and P for phase noise.

Consider a pulsed laser output with $\langle F \rangle = 0.5$ being used for nonlinear optical imaging such as SHG or THG microscopy, it is important to know how the low fidelity value affects signal intensity. In the most common case, phase fluctuations, SHG/THG decreases to $\frac{1}{2}$ or $\frac{1}{4}$ of the expected value for noiseless pulses. In the rare case of large spectral jitter, SHG/THG would decrease by a factor of $\sqrt{2}$ or $\frac{1}{2}$. In the case of mixed phase and amplitude noise, SHG/THG signal would be reduced by a factor of ~ 0.6 or $\sim 1/3$.

Fidelity measurements are also possible for pulse trains that do not average to Fourier-limited pulses. If the ensemble of laser pulses being measured has a net positive chirp, the MIIPS trace shifts to a negative chirp value. The opposite sign results because the maximum SHG is obtained when the net chirp of the laser is compensated by the chirp introduced by MIIPS. Numerically shifting the SHG intensity scan so that at all wavelengths the maximum SHG is centered at zero dispersion results in a plot similar to the MIIPS data shown in Figs. 1(a and b), from which a value for fidelity can be easily obtained. Fidelity measurements can also be obtained for lasers having a combination of linear chirp and third order dispersion (TOD). TOD causes a MIIPS trace to appear as a diagonal feature [17, 18], as shown in Fig. 5 (middle column). We find in Fig. 5 that if high order dispersion is uncorrected, then values for positive $\langle F_+ \rangle$ and negative $\langle F_- \rangle$ chirp are quite different; however, simply shifting each spectrum to zero dispersion yields the correct value for fidelity. It should be clear that any combination of linear chirp and TOD can be easily treated by shifting as shown in Fig. 5 (right column) to obtain reliable fidelity measurements. If higher-order phase distortions are present it is necessary to measure and compensate these distortions using iterative MIIPS [17, 18] or other pulse shaper based method capable of compensating arbitrary phase distortions. Note that the MIIPS average spectral phase measurement and compensation are not affected by noise. The reported pulse duration in the commercial MIIPS software, which takes into account the laser spectrum, would be underestimated in the case of a laser with low fidelity. This highlights the value of the proposed fidelity measurement.

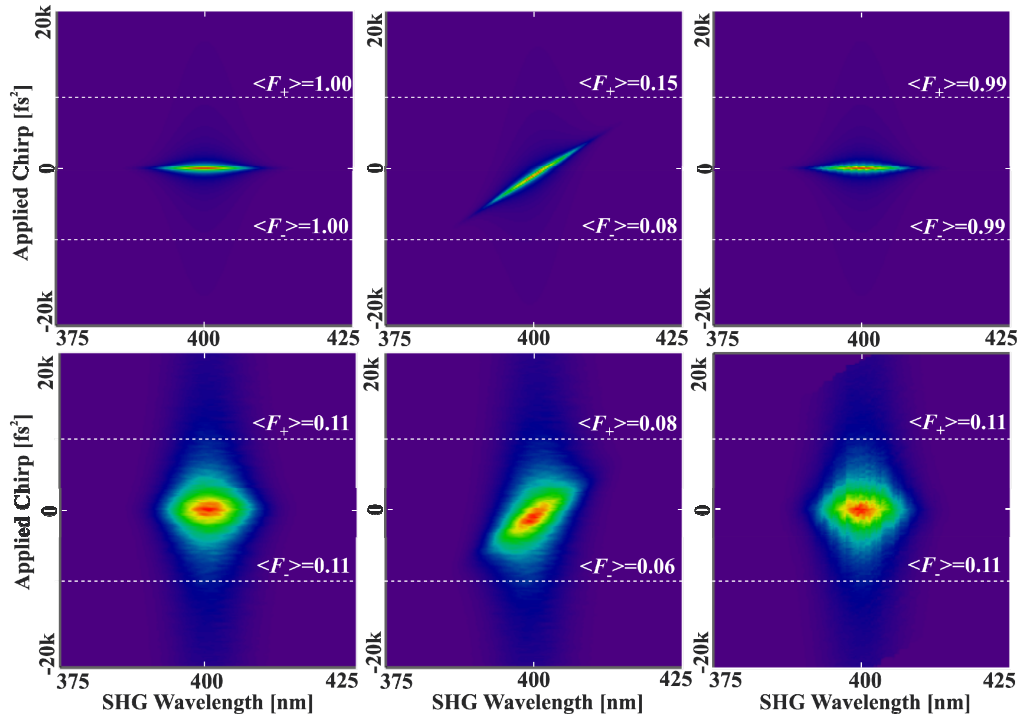


Fig. 5. 2D MIIPS traces for an ensemble of random pulse with average phase distortion 900fs^2 and $2.7 \times 10^4 \text{fs}^3$ starting with 30fs TL pulses. Chirp is scanned $\pm 20000\text{fs}^2$ (vertical axis), and the spectral range (horizontal axis) is 375nm to 425nm . First row illustrates coherent pulses with unit fidelity. Second row is for random pulses with average pulse duration 300fs . First column for no dispersion, second column with dispersion, and third column obtained by numerically shifting spectral line to zero chirp. The dashed white lines correspond to $\pm 9000\text{fs}^2$. Each simulation corresponds to 1000 random pulses, each measured as a function of 500 different chirp values.

4. Experimental measurements

We carried out fidelity measurements on a titanium sapphire oscillator (Micra, Coherent Inc), as shown in Fig. 6. After correction for dispersion using MIIPS we measure $\langle F \rangle$ values between 0.96 and 0.97. We attribute the less than perfect fidelity to spectral phase fluctuations based on the shape of the integrated SHG fidelity curve (see Fig. 6, bottom plots), which corresponds to spectral phase fluctuations as illustrated in Fig. 3 middle. We also include measurements obtained when the same oscillator had unstable temperature control of the sapphire crystal; in that case the fidelity value was smaller. Note that when a laser source is close to unit fidelity limit, measurements of $\langle F \rangle$ require attention to spectral phase, detector saturation, background, and signal to noise especially for high chirp values. We find that the high-chirp asymptotic condition should be near $\phi'' = 4\tau_c^2$, where the SHG intensity drops by approximately one order of magnitude compared to the chirp-free pulse. In the case of a low intensity laser, for which the signal to noise ratio (SNR) for Fourier-limited pulses is 1:1, the SNR at the asymptote would drop to 1:10. A fidelity measurement with 10% accuracy requires SNR of 10:1. Improving the SNR by two orders of magnitude would require 10^4 measurements, equivalent to averaging 10 seconds on a 1kHz laser. For a typical oscillator with MHz repetition rate, fidelity values with $\sim 1\%$ accuracy are obtained in under a second. While fidelity can reveal several negative laser conditions, there are many others such as temporal jitter and carrier-envelope-phase changes that it was not designed to measure.

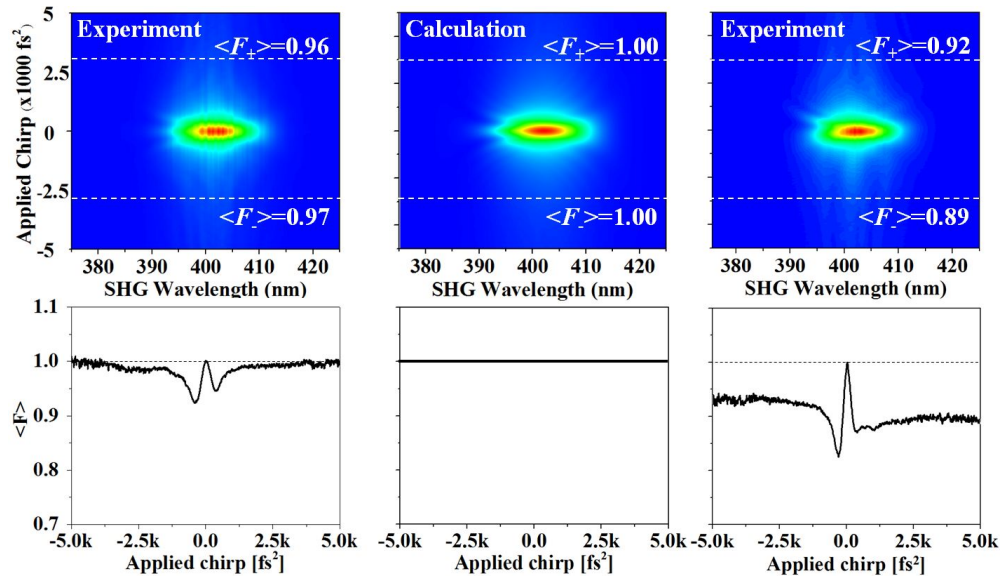


Fig. 6. Experimental 2D MIIPS trace for a titanium sapphire oscillator producing 27.5fs pulses (left), and the corresponding calculated MIIPS trace assuming perfect coherence (middle). (Right) Experimental 2D MIIPS trace for the same laser with destabilized temperature control. Bottom, fidelity curves based on integrated SHG intensity corresponding to each case above.

5. Summary

To summarize, we propose the measurement of a parameter based on the dependence of an integrated nonlinear optical process on spectral phase, such as chirp, in order to determine the expected performance of an ultrafast laser source. The proposed measurement is particularly useful when performance is compromised by random noise in the laser. The measurement proposed bypasses autocorrelation based methods which are dominated by the coherence time of the pulses leading to a coherent spike. The fidelity parameter $\langle F \rangle$ is expressed in terms of values that can be practically measured in the laboratory. Experimental measurements on a commercial titanium sapphire oscillator are also presented. Fidelity measurements could be used to benchmark the performance of ultrafast lasers. In addition, fidelity can be measured actively and used as a feedback for active improvement of a laser source. We find one is able to determine the physical mechanism responsible for noise by examining the shape of the fidelity curve as seen in Fig. 3. We provide a direct correlation between the fidelity value and the expected attenuation of a second order process such as two-photon excited fluorescence, SHG, three-photon excited fluorescence, or THG, given a source that has reduced fidelity. In future publications we will demonstrate fidelity curves measured for fiber lasers and for amplified titanium sapphire lasers.

Acknowledgments

The authors wish to thank Professors Rick Trebino and Günter Steinmeyer for bringing to our attention the problem of characterization of noisy laser sources. We are also grateful for discussions about this work with Professor Frank Wise, Dr. Bai Nie and Dr. Rachel Glenn.